Comparisons of ECH Plasmas with and without Symmetry in the Helically Symmetric Experiment*

S. P. Gerhardt, A. Abdou, A.F. Almagri, D.T. Anderson, F.S.B. Anderson, D. Brower[1], J. Canik, C. Deng[1], W. A. Guttenfelder, K. Likin, P. H. Probert, S. Oh, J. Tabora, V. Sakaguchi, J. Schmitt, J.N. Talmadge, and K. Zhai.

The HSX Plasma Laboratory, University of Wisconsin-Madison, USA
*[1] Electrical Engineering Department, University of California, Los Angeles, USA*

Outline

- Overview of the Device.
- Studies of ECH Absorption.
- Studies of Stored Energy and Central T_e vs. Launched Power and Machine Configuration.
- Studies of Ion Flow Damping.
- Evidence of Direct Loss Orbits and Impurity Flow with Broken Symmetry.

The Helically Symmetric Experiment

|B|

R/a ~8

(R/a)$_{eff}$~400
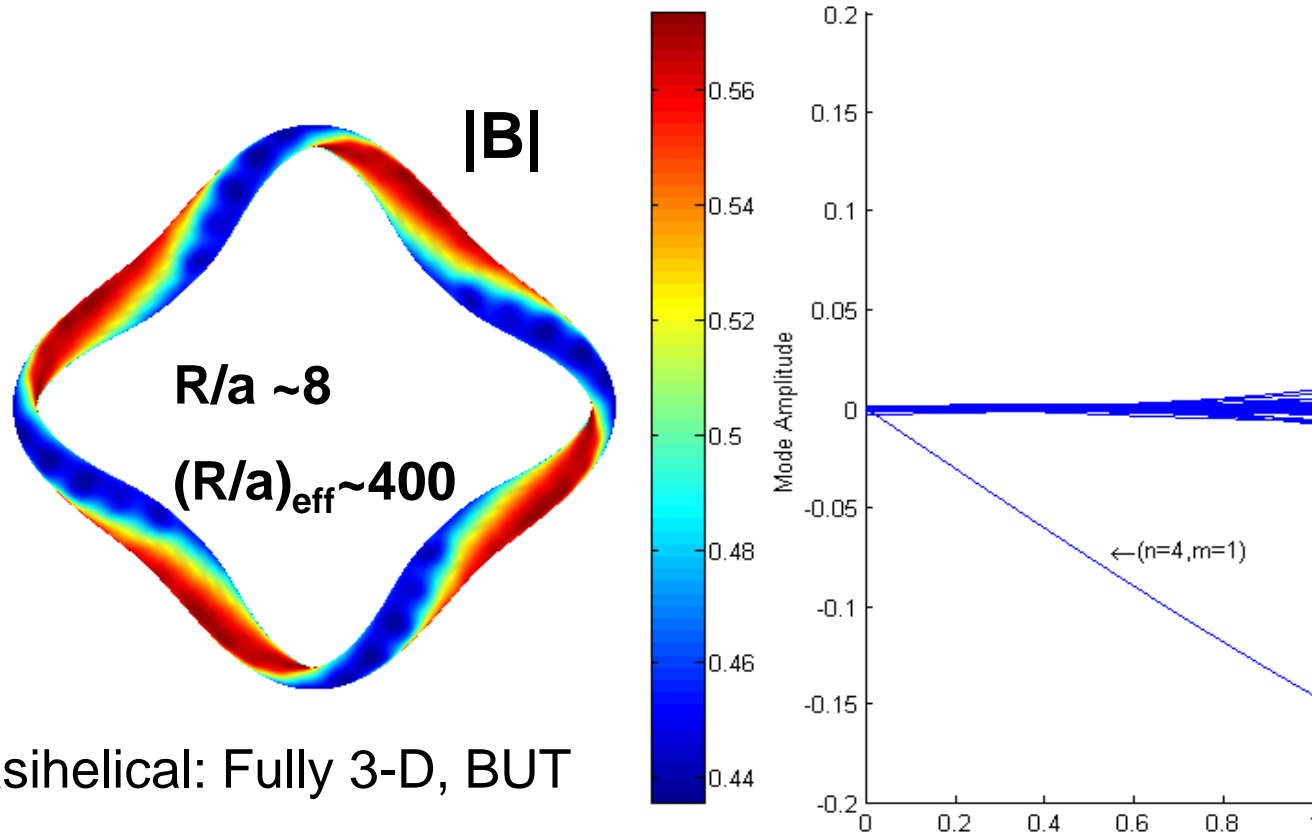
Quasihelical: Fully 3-D, BUT

Symmetry in |B| : $B = B_0\left[1 - \varepsilon_h \cos(N\phi - m\theta)\right]$

In straight line coordinates $\theta = \iota\phi$, so that $B = B_0\left[1 - \varepsilon_h \cos(N - m\iota)\phi\right]$
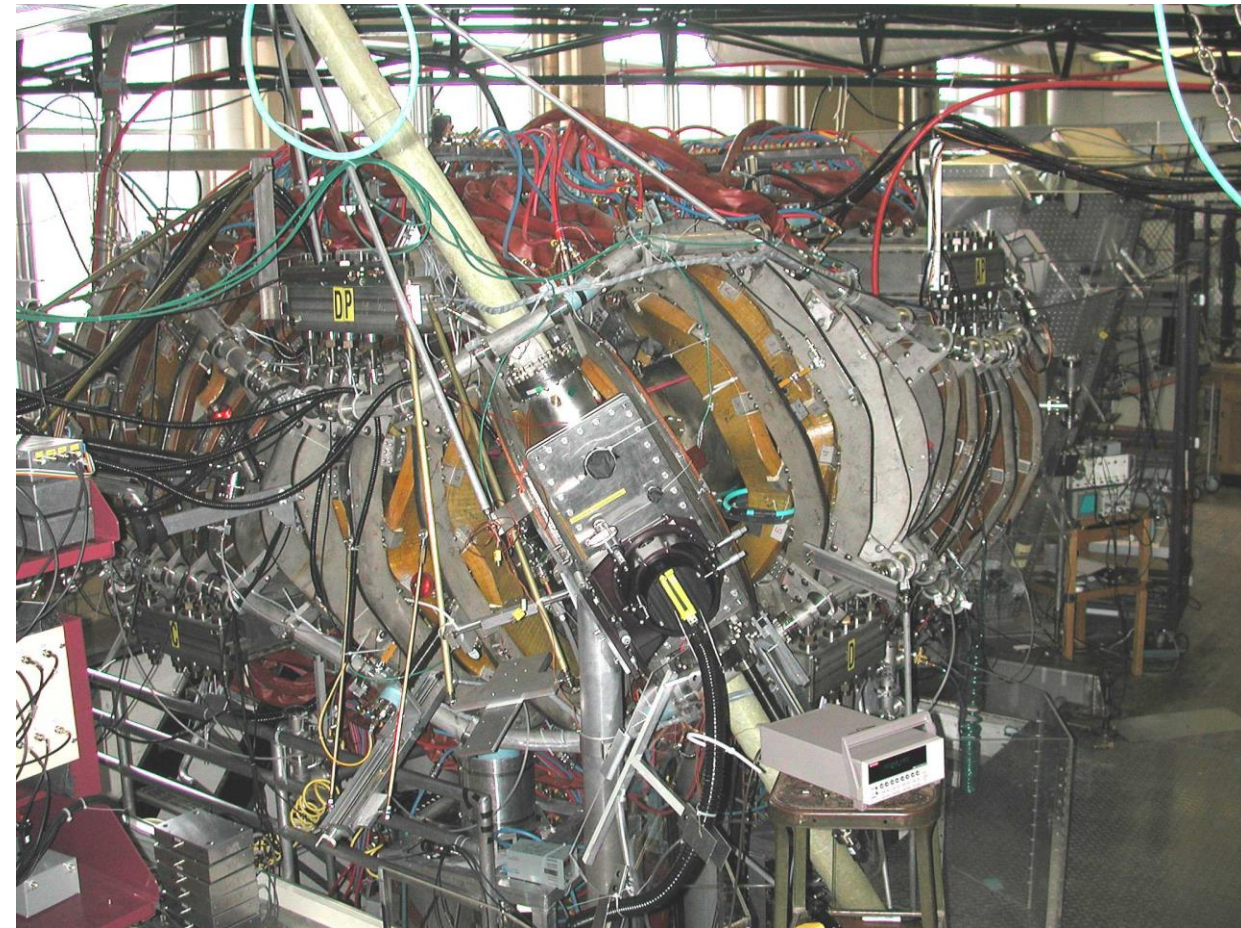
In HSX: N=4, m=1, and ι ~ 1

$\iota_{eff} = \text{N-m}\ \iota = 1/q_{eff} \sim 3$

ICC Meeting, Seattle, 2003

The HSX Device

Current Operational Parameters of HSX

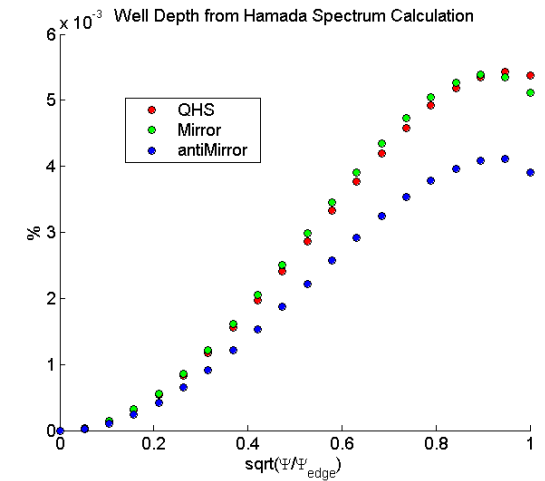|	
Major Radius	1.2 m
$\langle r \rangle$	0.12 m
Volume	~.37 m^3
Field periods	4
ι_{axis}	1.05
ι_{edge}	1.12
Coils/period	12
B_0	.4-.6 T
ECH Pulse length	Up to 50 msec.
Heating Power	Up to 100kW

Three Different Configurations of HSX

Different Magnetic Field Spectra…

QHS

Mirror

antiMirror
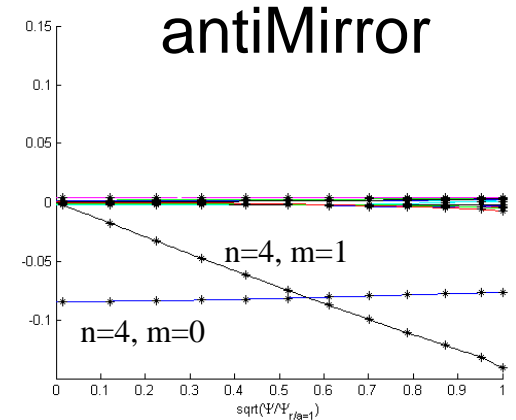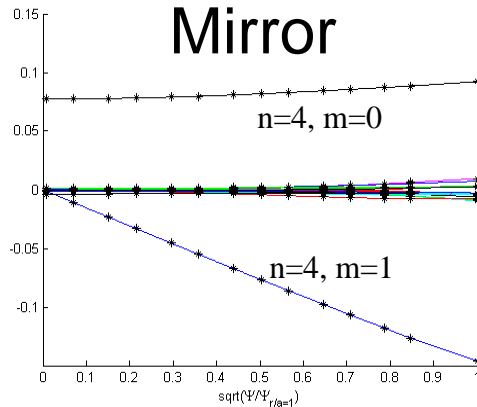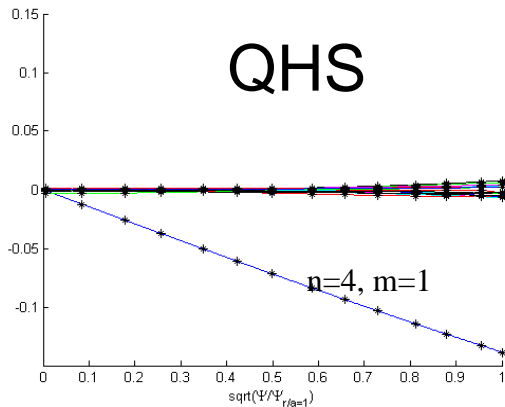
…but other properties are similar
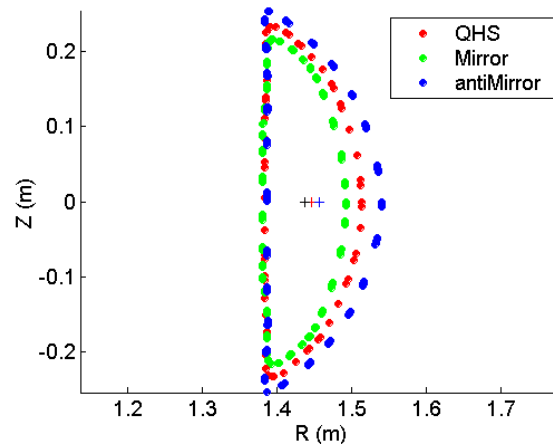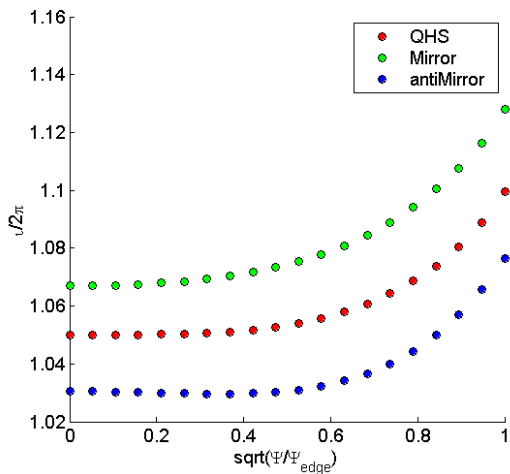
Diagnostic Set

|	
Diamagnetic Loop	Stored Energy, Absorbed Power
Thomson Scattering (1 channel, upgrading to 10)	T_{eo}, soon $T_e(\Psi)$
9 chord Microwave Interferometer	n_e Profile and Fluctuation UCLA
1-meter UV/Vis. CCD spectrometer	Impurity Levels, Temperature, and Flow
Microwave Antennas (x6)	Absorbed Power
Bolometer (1 channel, upgrading to 2)	Radiated Power
Langmuir Probes	Edge Density, Ion Flows, Turbulence
H_α arrays, toroidal and poloidal	Neutral Density and Recycling
CdZnTe PHA system	High Energy Electron Population
PMT Monochromaters	Fast Impurity Monitoring
SXR Monitors (3 channels, upgrading to 20 channel linear array)	$T_e(t)$ by 2 Filter Method, Moving Toward SXR Tomography.
4 Channel ECE Radiometer	$T_e(\Psi,t)$

Excellent Absorption of ECH Power in HSX Plasmas

EC Heating in HSX

- Microwave power (up to 100 kW at 28 GHz) is used for neutral gas breakdown followed by heating of plasma at the second harmonic of electron cyclotron frequency.

- Linear polarized beam with $\mathbf{E} \perp \mathbf{B}$ is launched from the low magnetic field side and it is focused on the plasma center in a spot of 4 cm in diameter.
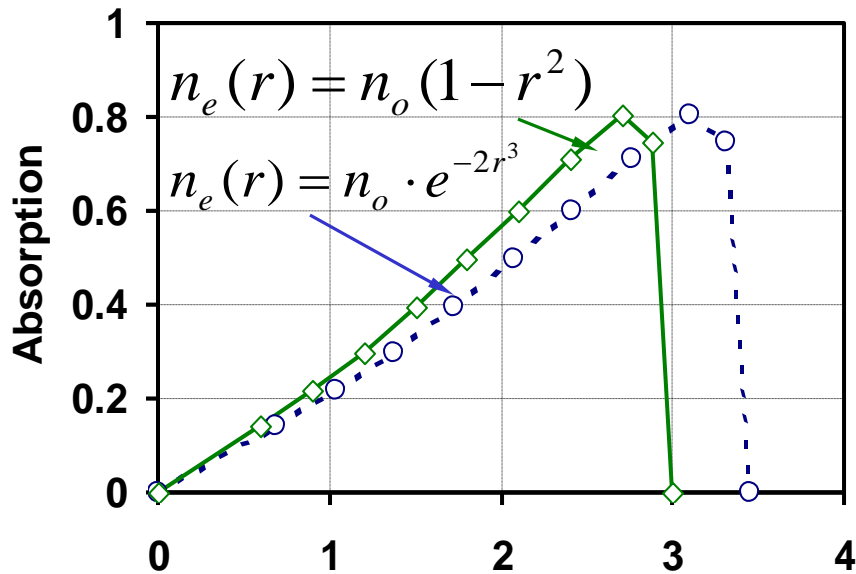

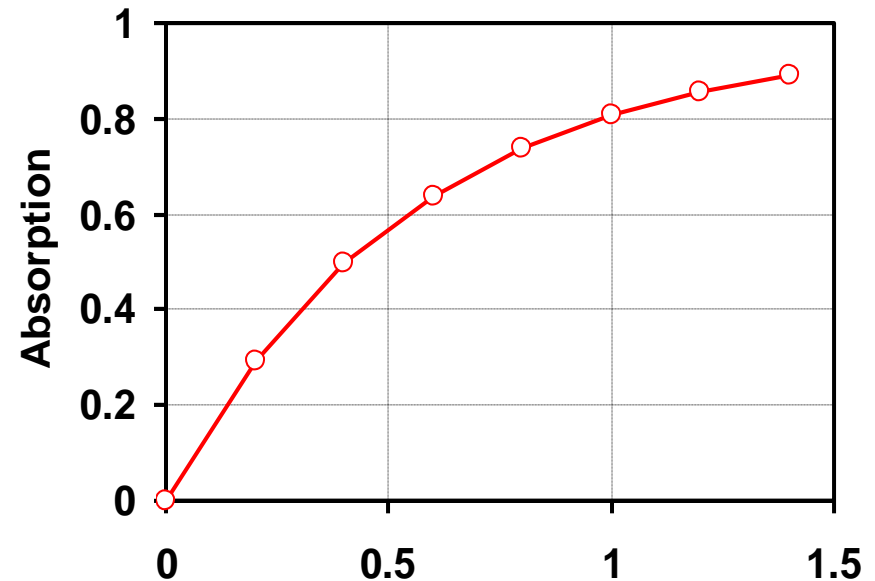Vertical cut
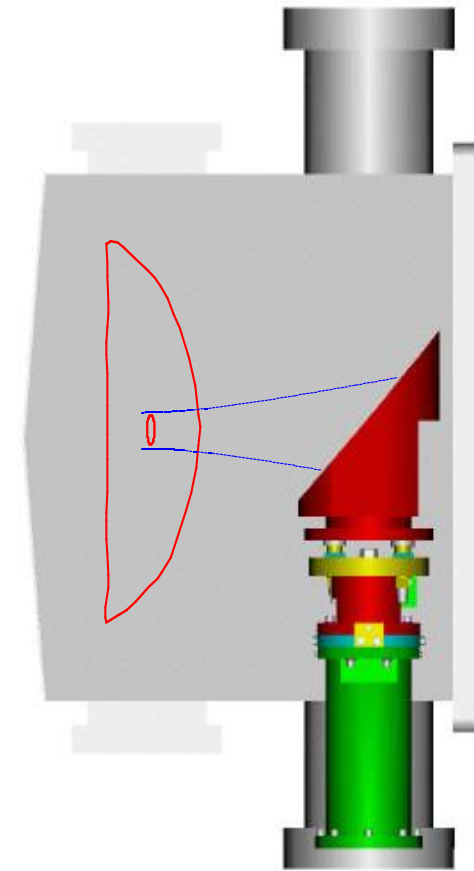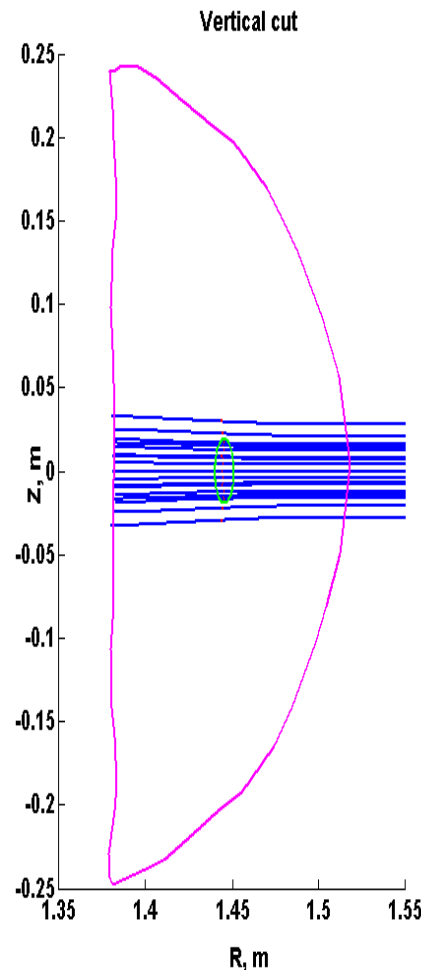
Ray Tracing Predicts Approximately 40% Single Pass Absorption.

$T_e(0) = 0.4$ keV $B_o = 0.5$ T $n_e = 2*10^{18}$ m^{-3}

$$n_e(r) = n_o(1 - r^2)$$

$$n_e(r) = n_o \cdot e^{-2r^3}$$

Absorption

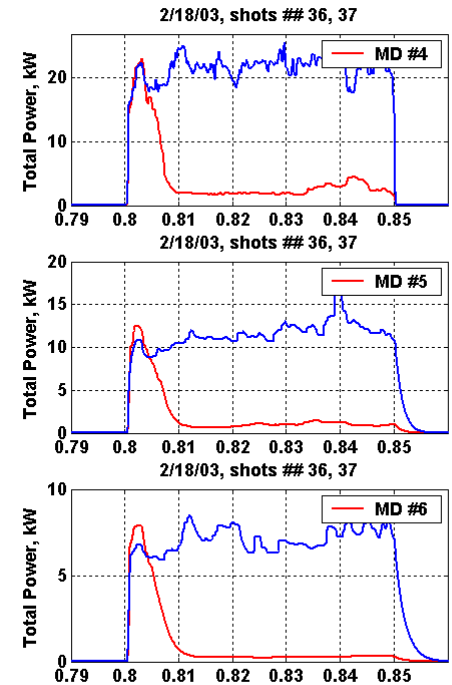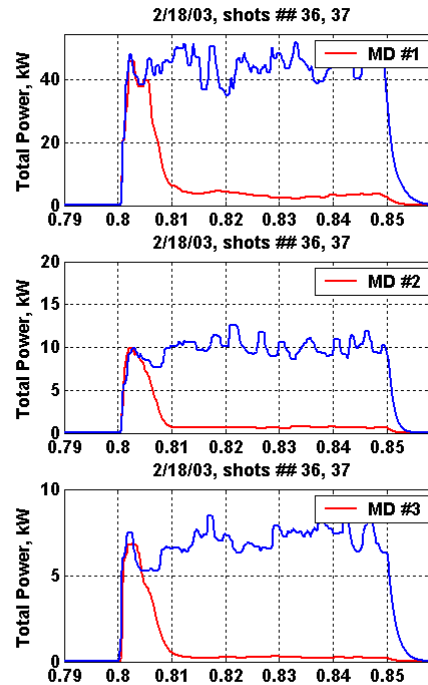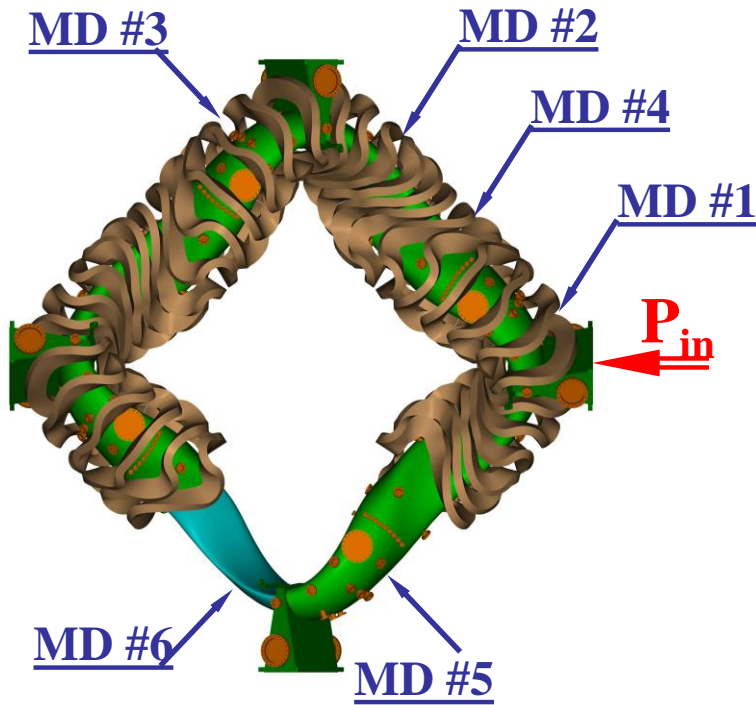Line average density, 10^{18} m^{-3}

Absorption

Central temperature, keV

- Predicted first pass absorption increases with density and temperature.

- Approximately 40% single pass absorption predicted for $n_e = 1.5 \times 10^{12}$ cm^{-3}, $T_e = 500$eV

ICC Meeting, Seattle, 2003

Measured ECH Absorption in HSX is Much Better than the Single Pass Prediction.

MD #3 MD #2

MD #4

MD #1

P_{in}

MD #6

MD #5

2/18/03, shots ## 36, 37 — MD #1
2/18/03, shots ## 36, 37 — MD #4
2/18/03, shots ## 36, 37 — MD #2
2/18/03, shots ## 36, 37 — MD #5
2/18/03, shots ## 36, 37 — MD #3
2/18/03, shots ## 36, 37 — MD #6

(plots: Total Power, kW vs time 0.79–0.85)

- Microwave detectors show ≈90% absorption in QHS and Mirror, for $.3 \times 10^{11} < n_e < 2 \times 10^{12}$ cm^{-3}.

- Absorption drops to ≈50% in antiMirror.

In shot #36:

Good Absorption

$n_e = 1.5 \times 10^{18}$ m^{-3}

$W_E = 22$ J

In shot #37:

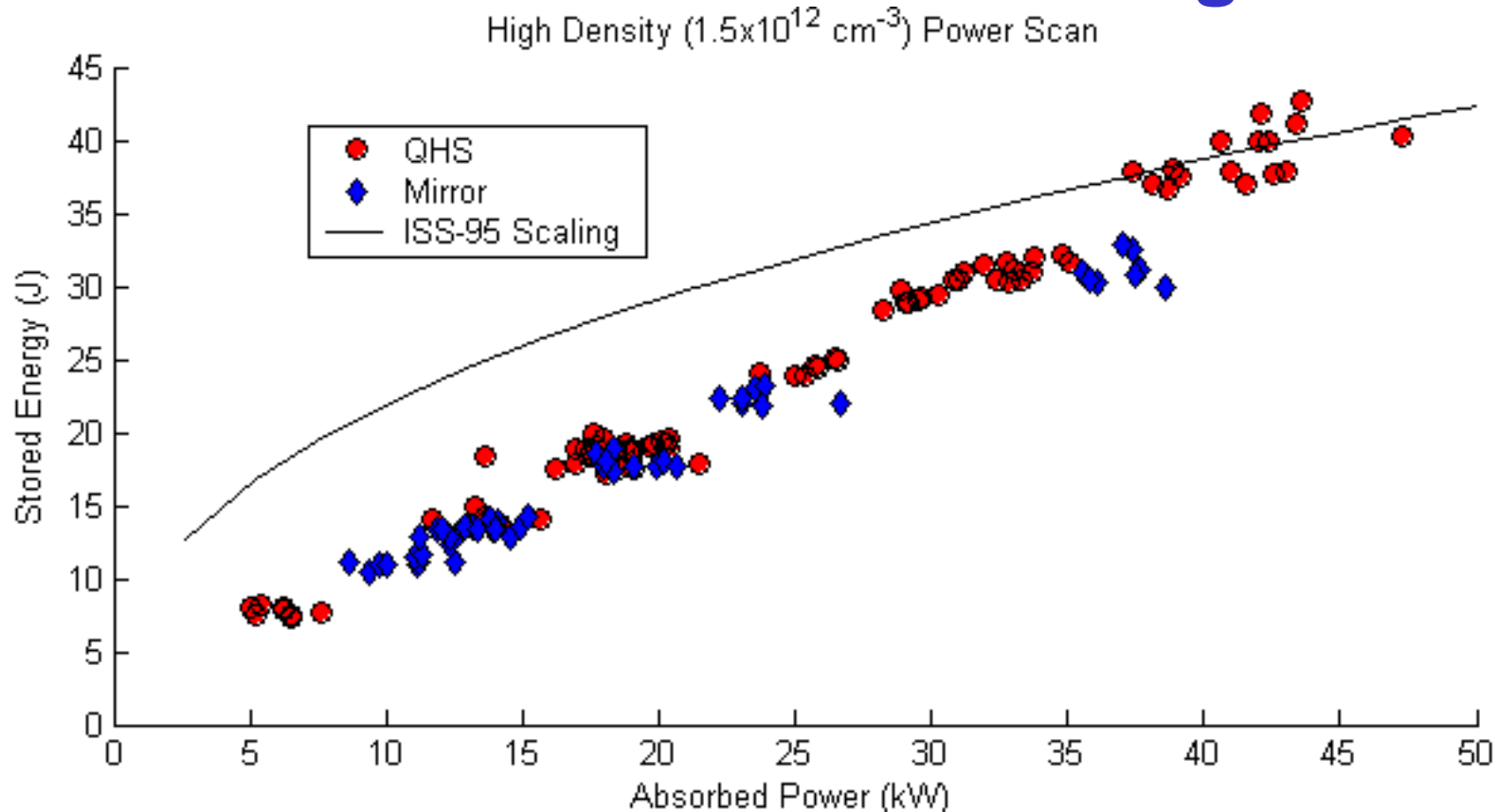Vacuum Level

$n_e = 3.1 \times 10^{18}$ m^{-3}

$W_E = 1.6$ J

HSX

# HSX Meets ISS-95 Scaling at 90kW Launched Power, with Electron Temperatures in Excess of 600eV.

Stored Energy Increases Linearly with Heating Power in QHS and Mirror Configurations.

High Density (1.5×10^{12} cm^{-3}) Power Scan

- Stored energy and absorbed power from the diamagnetic loop.
- Experiments done at a density of 1.5×10^{12} cm^{-3}.
- Confinement matches ISS-95 scaling at higher power levels, but no power degradation yet observed ($W = P_{abs}\tau^{ISS-95} \propto P^{-.4}$).

# The Central Electron Temperature Rises Linearly with Absorbed Power.

Central Electron Temperature

Legend:
- Mirror, High Density (1.5×10^{12} cm^{-3})
- QHS, High Density (1.5×10^{12} cm^{-3})
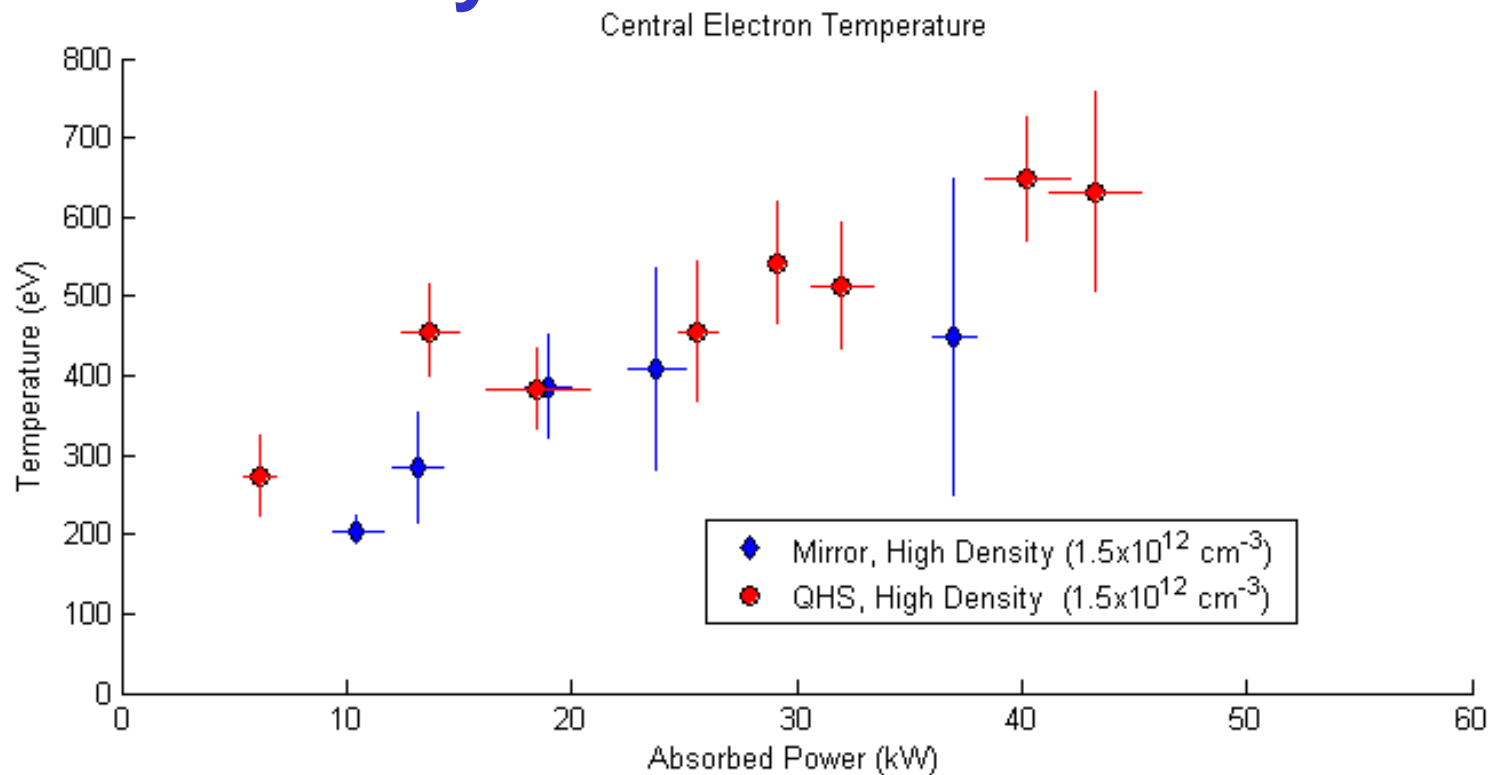
- Experiments done at a density of 1.5×10^{12} cm^{-3}.

- Each data point represents an average of a number of discharges.

- Neoclassical thermal conductivity not expected to be important at these temperatures and densities.
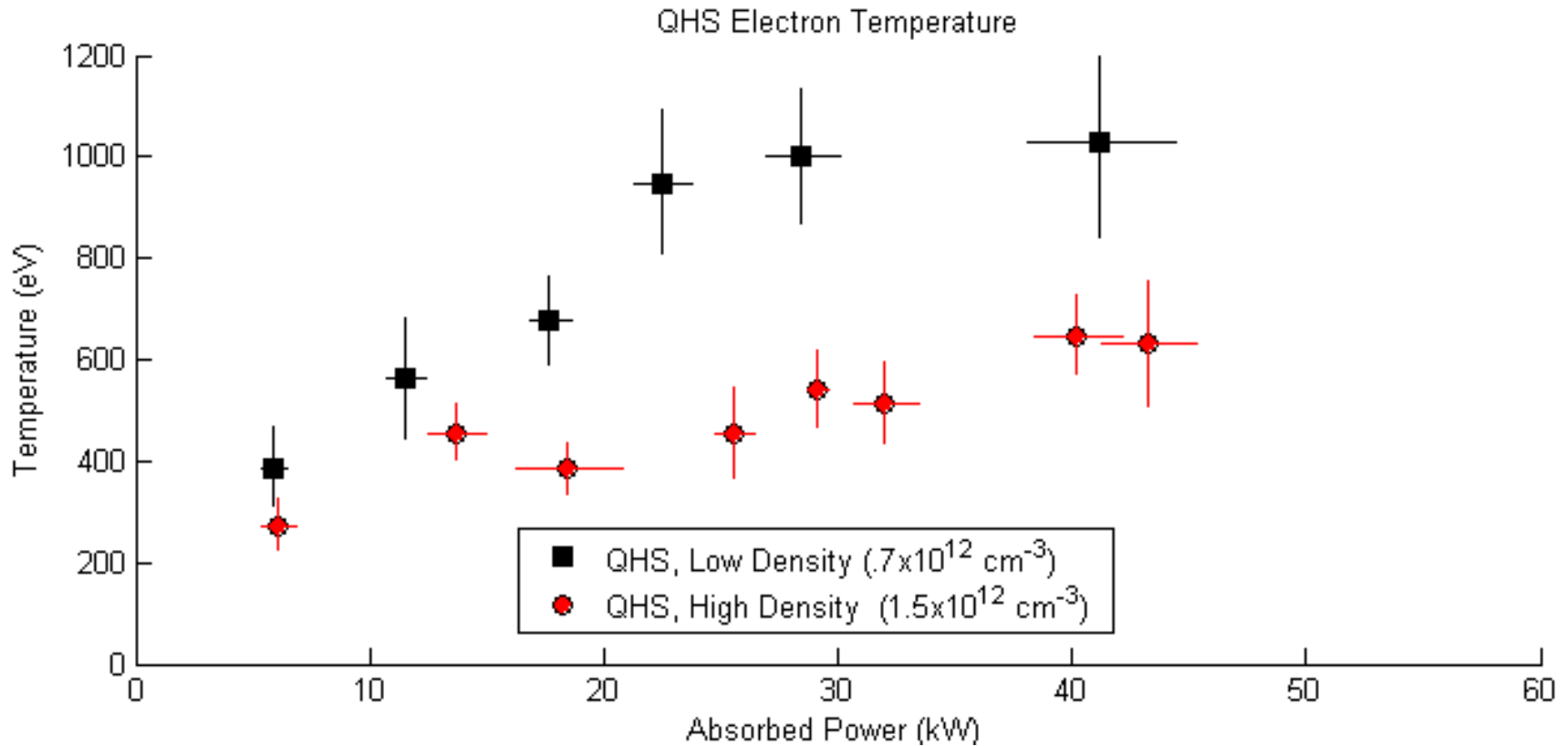
Radiated and Absorbed Power Rise Linearly with Input Power.
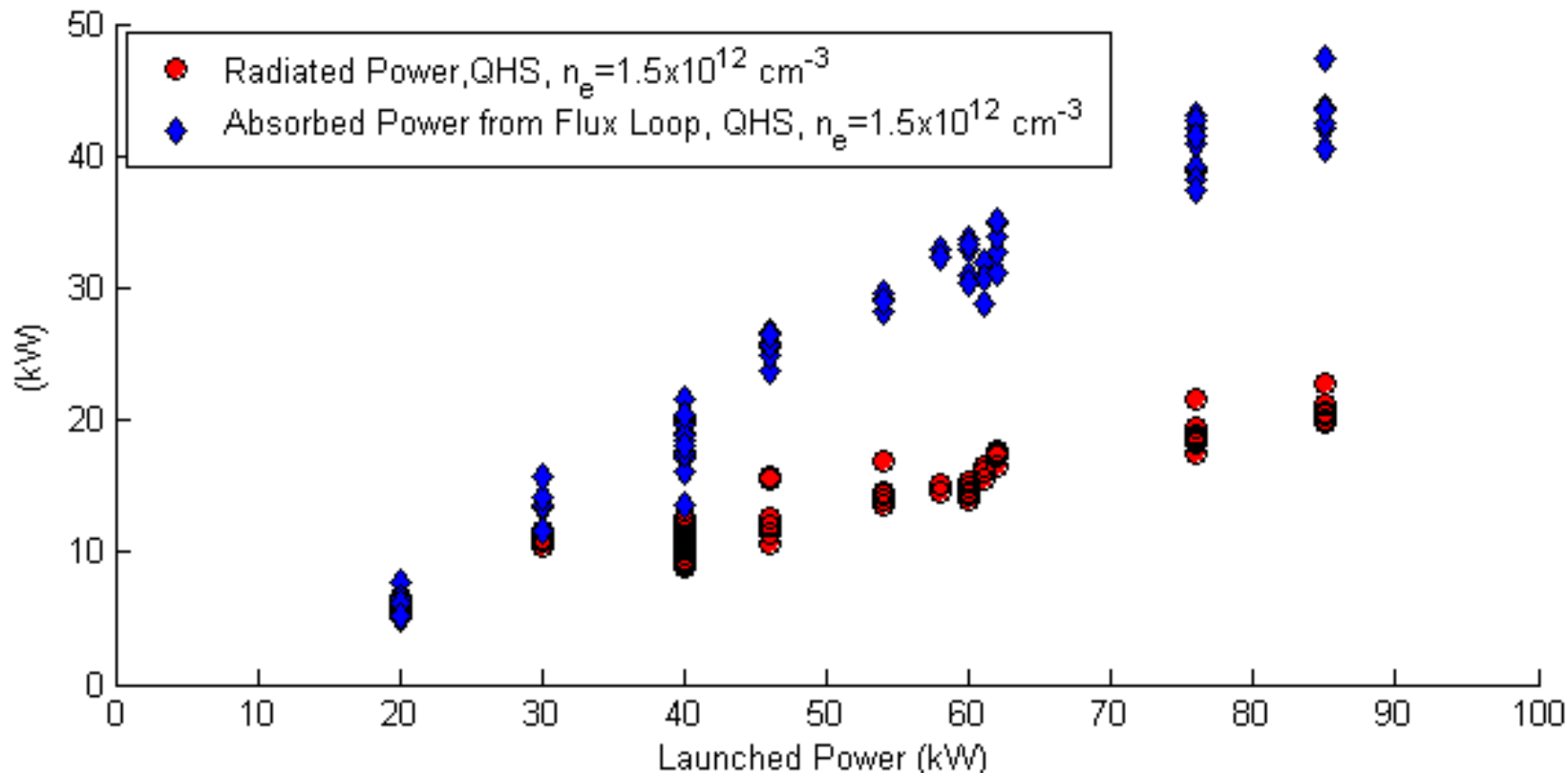
- Radiated power measured by single bolometer, with assumption of toroidal symmetry.
- Radiated power $\approx$ 25% of launched power.
- Flux loop absorbed power $\approx$50% of launched power.

Electron Temperature Reaches 1keV at 40kW Absorbed Power and Low Density
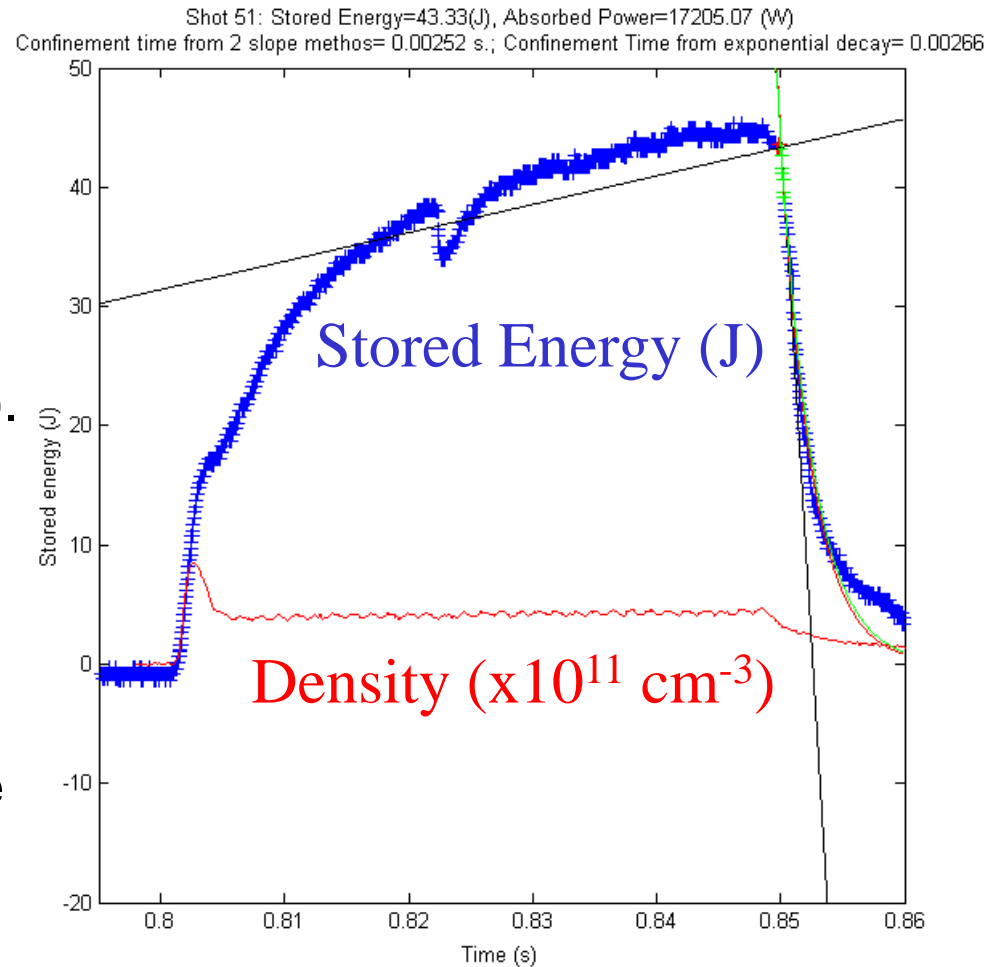

QHS Electron Temperature

- Each data point is an average of several similar discharges.
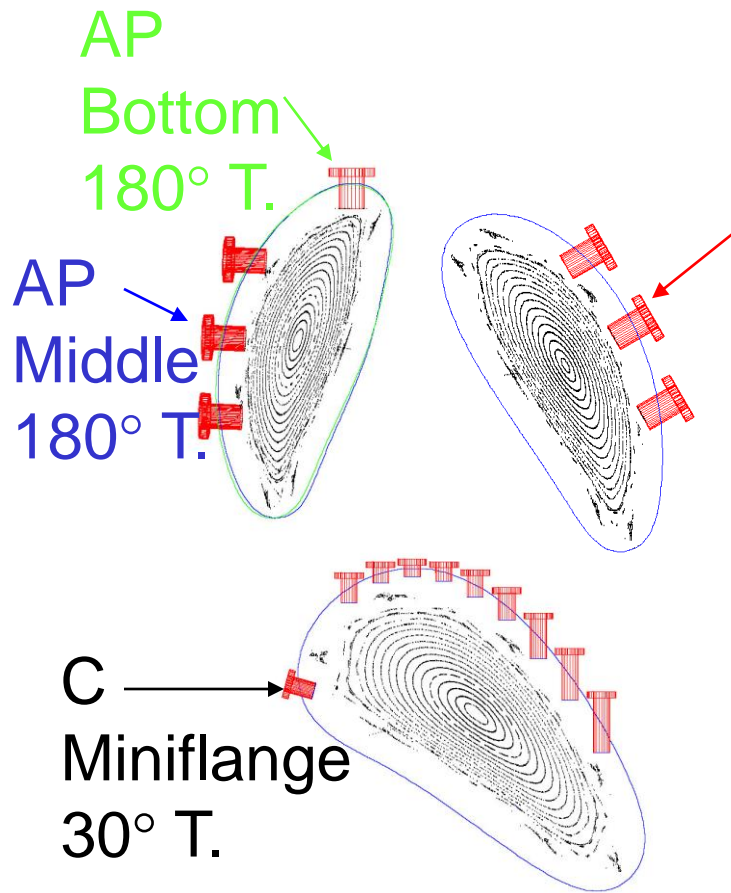- Tail population may impact Thomson scattering data and low density.

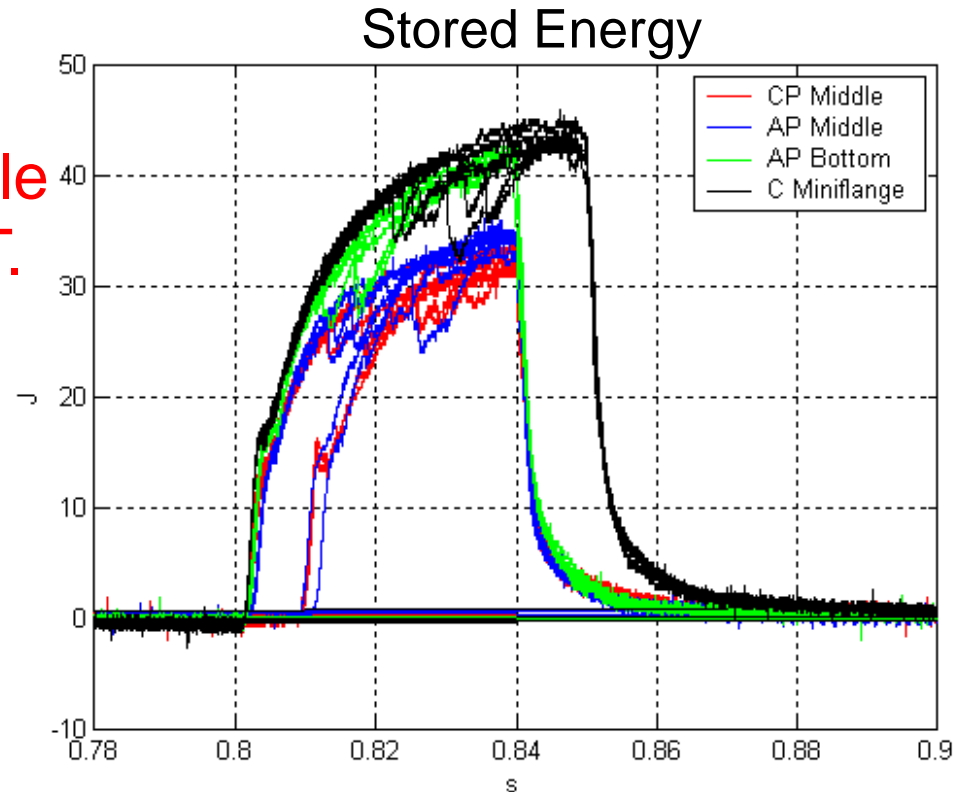# Best Performing HSX Plasmas are at Low Density, Slightly Inboard ECH Resonance.

■45kW ECH power launched, with approximately 17kW absorbed, as estimated by diamagnetic loop decay.

■Confinement Time of approximately 2ms (τ_{ISS-95}=.8ms).

■Access to these high performance discharges depend on gas fueling location.

■The previous power scans were done with non-optimum gas puffing.

Shot 51: Stored Energy=43.33(J), Absorbed Power=17205.07 (W)
Confinement time from 2 slope methos= 0.00252 s.; Confinement Time from exponential decay= 0.00266

Stored Energy (J)

Density (x10^{11} cm^{-3})

Stored energy (J)

Time (s)

HSX

Stored Energy Strongly Impacted By Puff Location.

AP Bottom 180° T.

AP Middle 180° T.

CP Middle 30° T.

C Miniflange 30° T.

Stored Energy

- All discharges at n_e=.4x10^{12} cm^{-3}, QHS, slightly inboard ECH resonance.

- Distance from the ECH location less important than the distance of the puffer from the axis.

# Reduction of Viscous Damping with Symmetry

Setup of the Damping Measurements

- Plasma rotation caused by a radial current drawn by an electrode inside the LCFS.

- Electrode can be switched on and off very quickly.

- Measure the induced flow with 6 tip Mach probes.

- Flow is measured in the region between the LCFS and the electrode.

- Measure the electric field with rake probes.
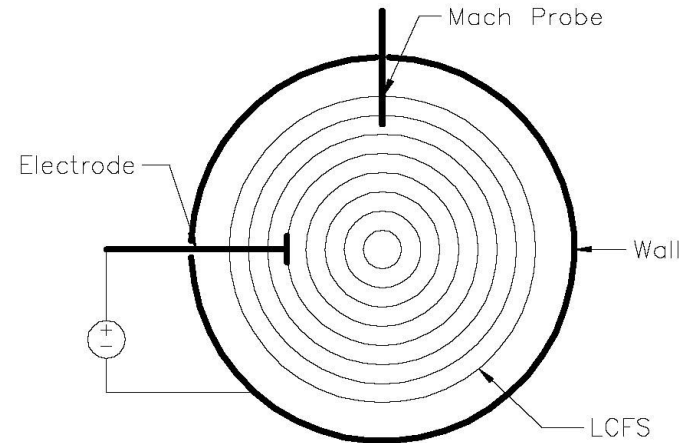
Example of Mach Probe Data
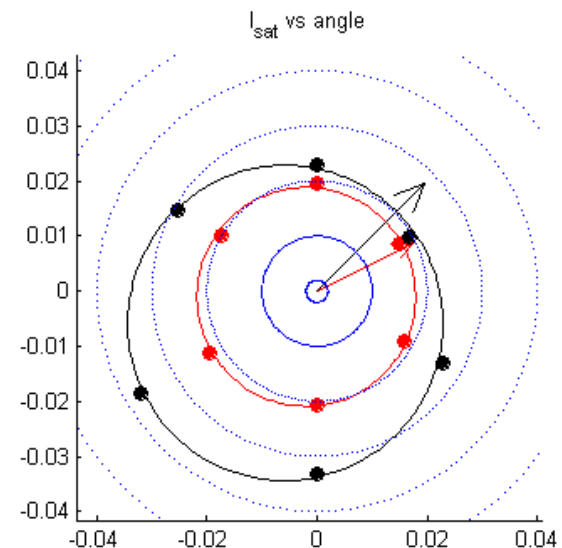
Longer Damping Time with Symmetry

- QHS flow rises more slowly to a larger value.

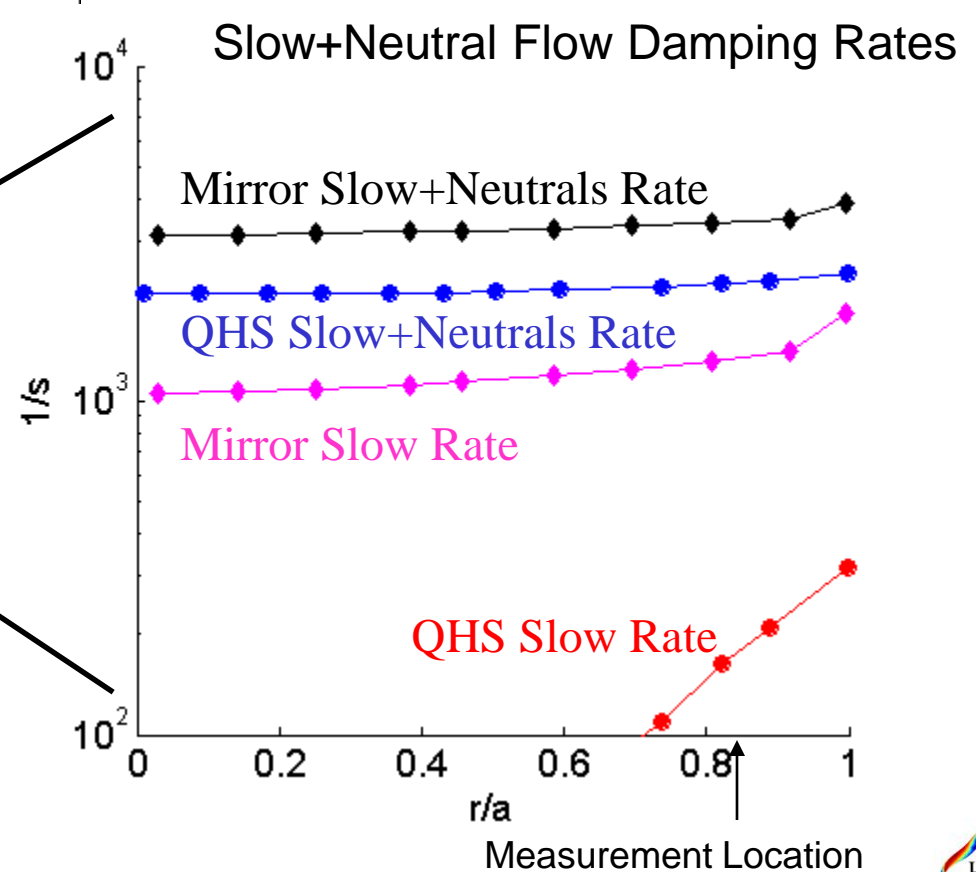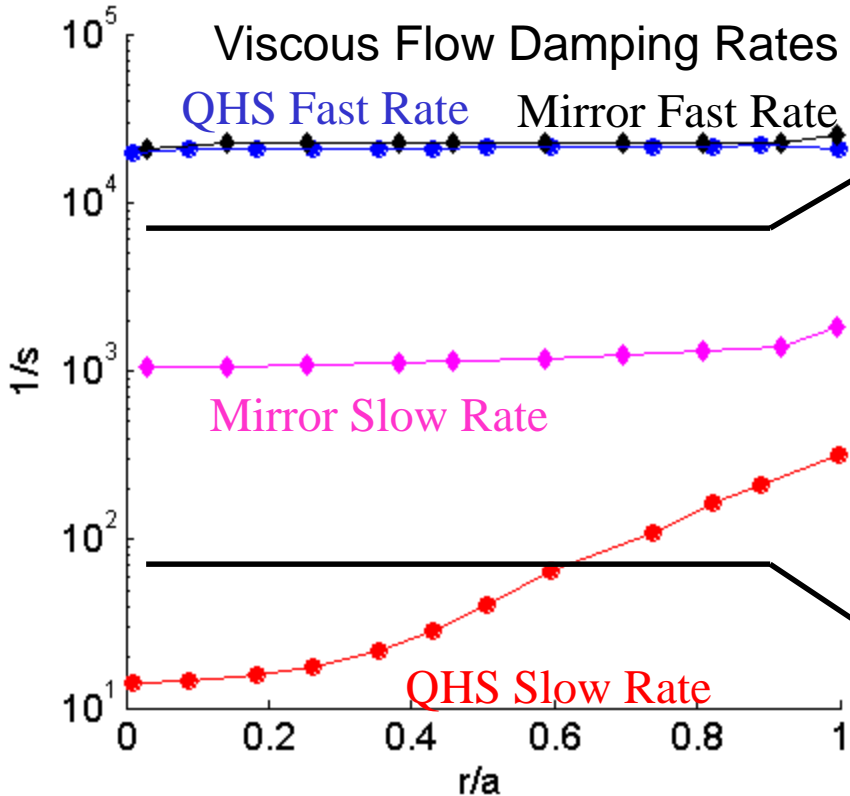- Normalized flow velocity as a figure of merit:

$$U_{norm} = M_\theta / I_{bias}$$

- Higher normalized velocity indicates reduced total damping

- Factor of 2 difference, consistent with modeling.

Mach Number — QHS — Mirror
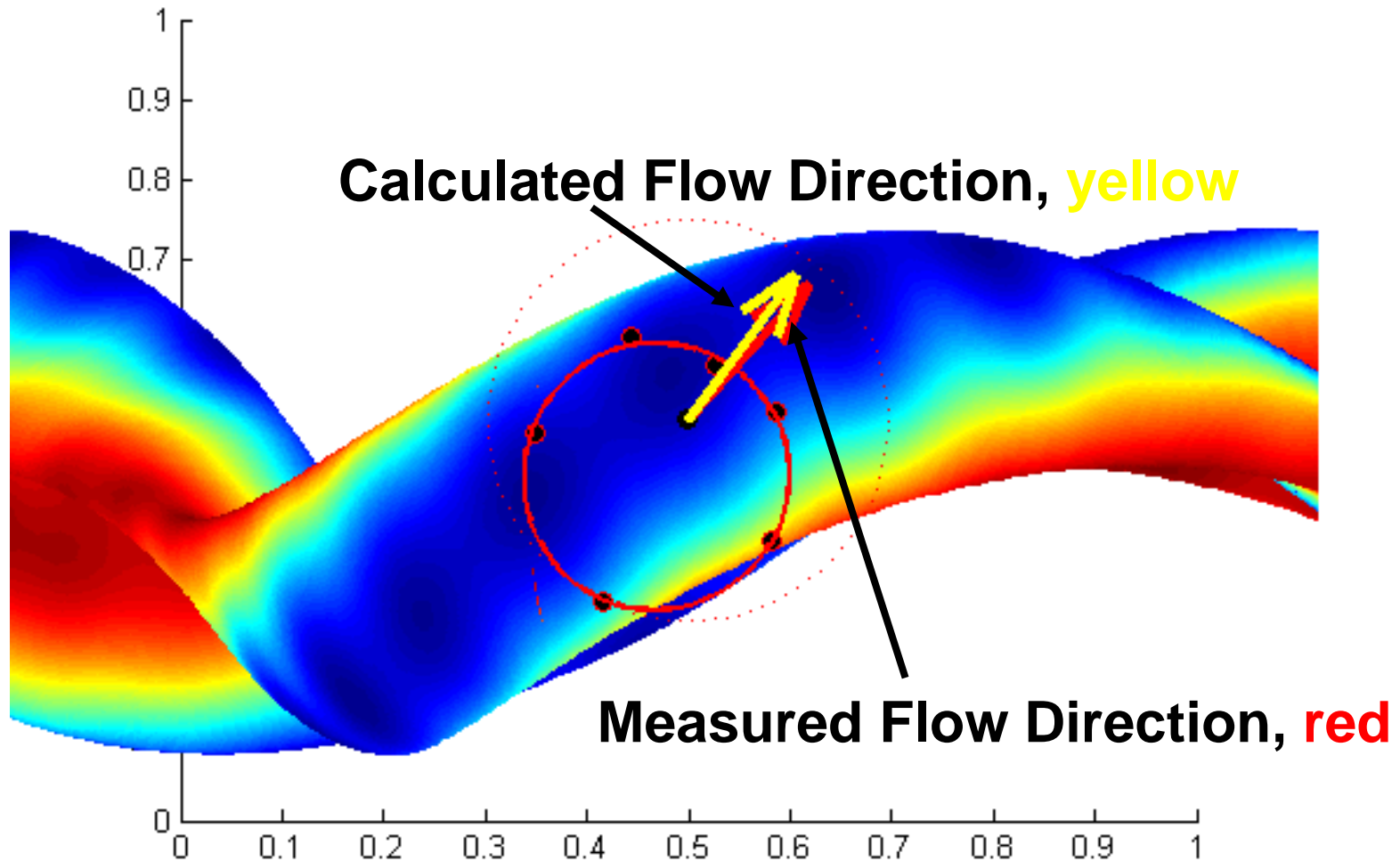
Floating Potential

Normalized Flow
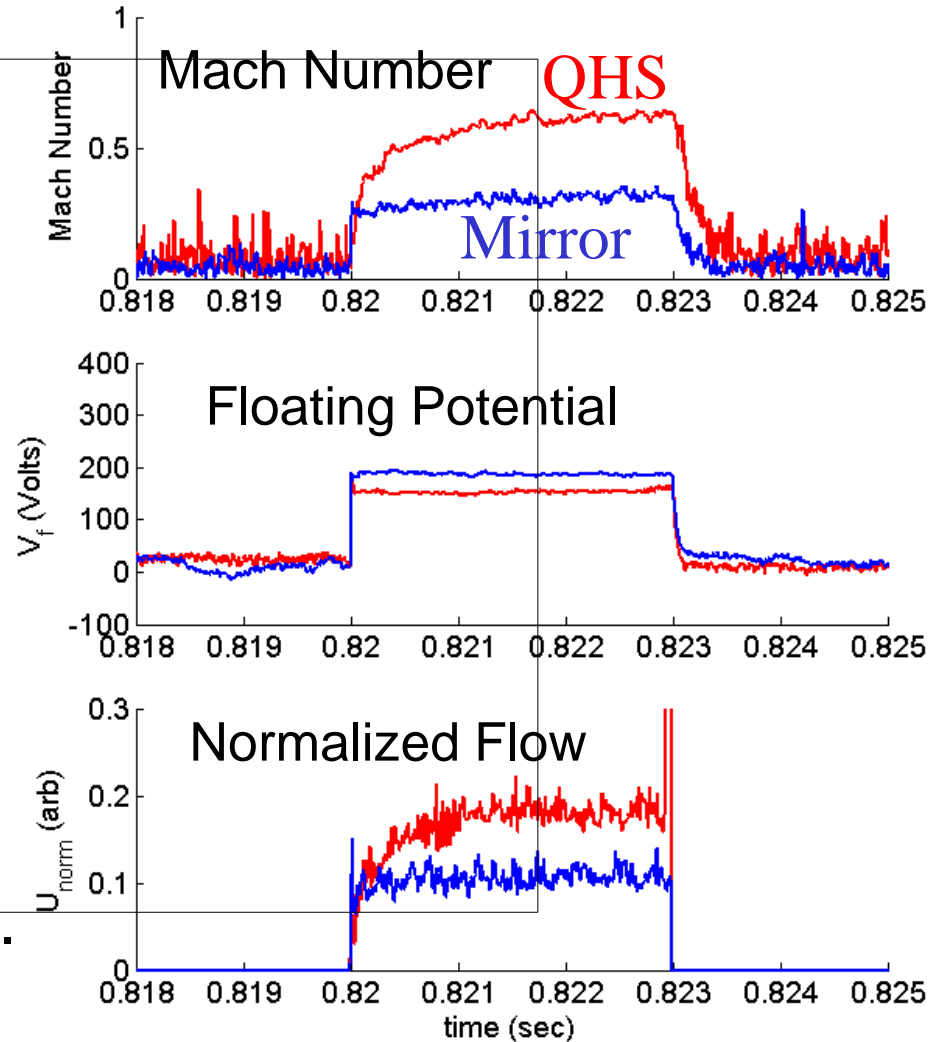
Damping Rates are in Agreement with predictions from Neoclassical Modeling.

Two damping rates on a surface, corresponding to two directions on a surface.

Neutral damping reduces the expected difference in the rates.

Viscous Flow Damping Rates

QHS Fast Rate   Mirror Fast Rate

Mirror Slow Rate

QHS Slow Rate

Slow+Neutral Flow Damping Rates

Mirror Slow+Neutrals Rate

QHS Slow+Neutrals Rate

Mirror Slow Rate

QHS Slow Rate

Measurement Location

This Modeling Makes Accurate Predictions For the Flow Direction.

Calculated Flow Direction, yellow

Measured Flow Direction, red

Evidence of Direct Loss Orbits With Broken Symmetry

Computations Show Reduced Direct Loss Orbits for QHS.

- 80° pitch angle electrons followed in Boozer coordinates.

- Launched on the outboard side of the torus as a point of minimum |B|.

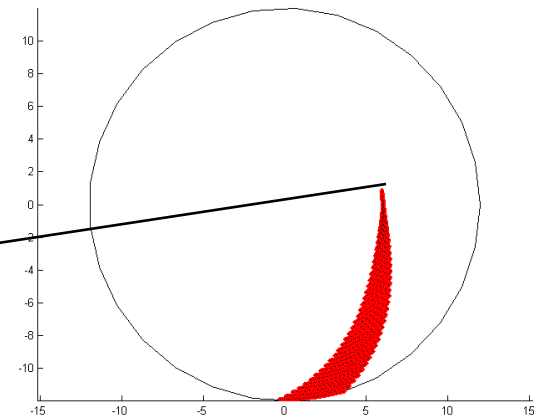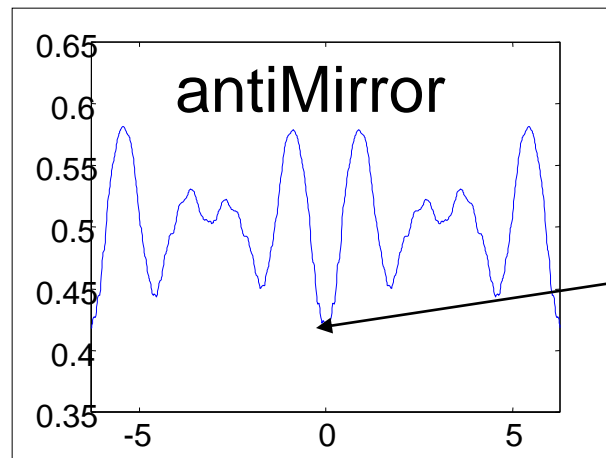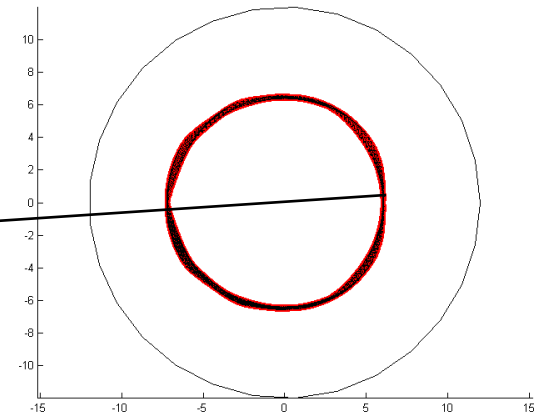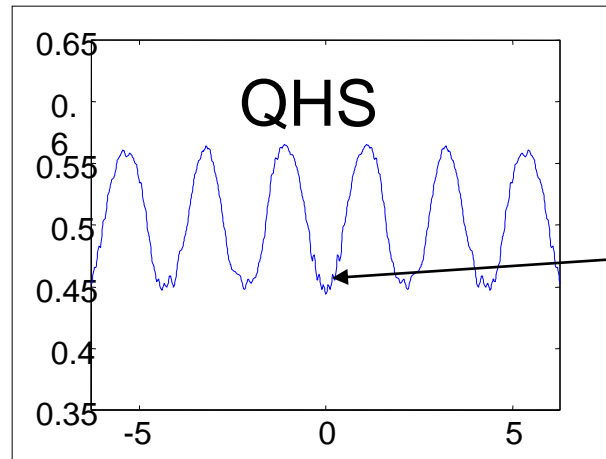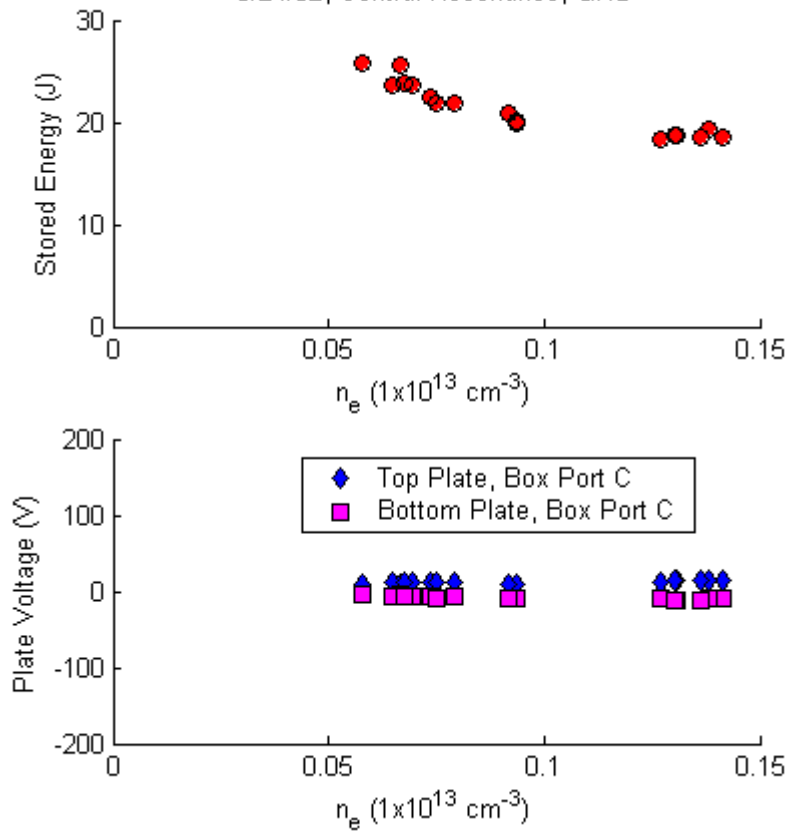- QHS orbit is a simple helical bananna; antiMirror orbit quickly leaves the machine.

Plate in grad(B) Drift Direction Measures a Very Negative Floating Potential in the antiMirror Configuration.

QHS

antiMirror
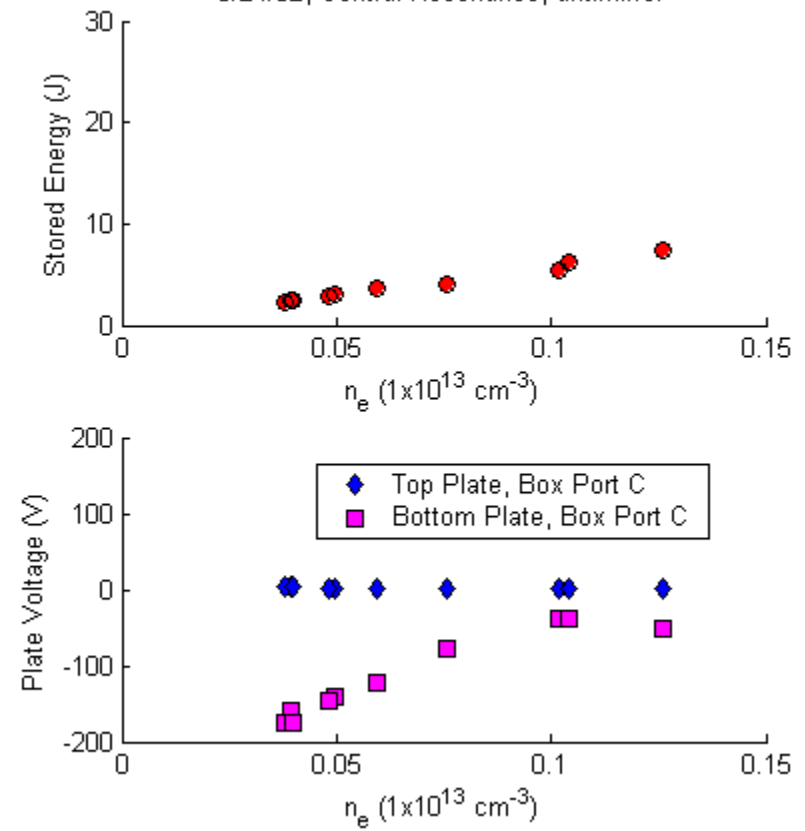
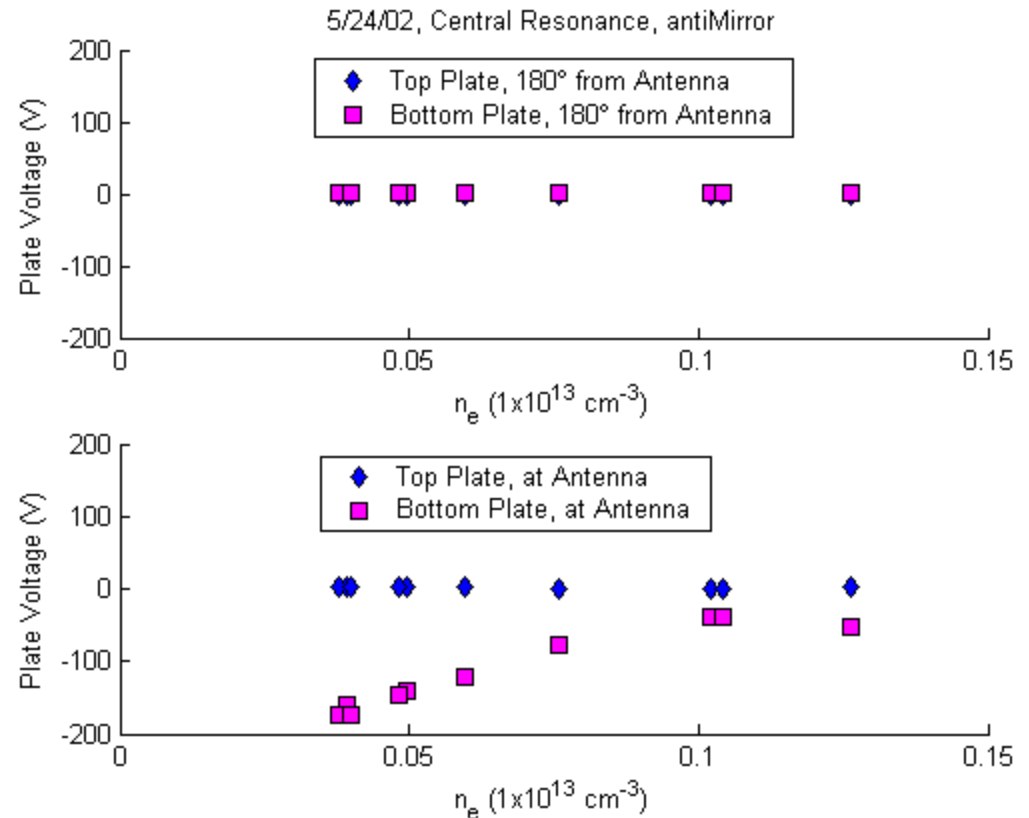# Plates Near the ECH Antenna Behave Differently than Those 180 Degrees Away

Plates 180° toroidally displaced show very little signal, no asymmetry.

Plates at the location of the antenna show the up/down asymmetry.

5/24/02, Central Resonance, antiMirror

- Top Plate, 180° from Antenna
- Bottom Plate, 180° from Antenna

Plate Voltage (V)

n_e (1×10^{13} cm^{-3})

- Top Plate, at Antenna
- Bottom Plate, at Antenna

Plate Voltage (V)
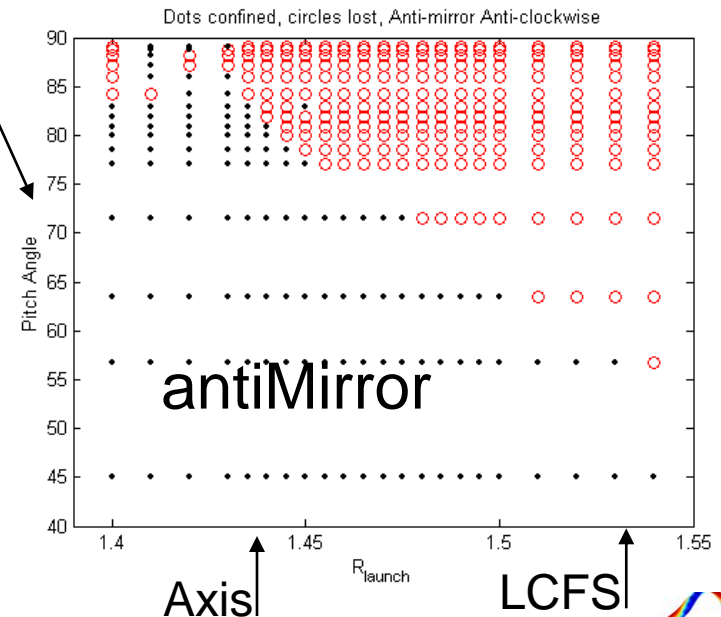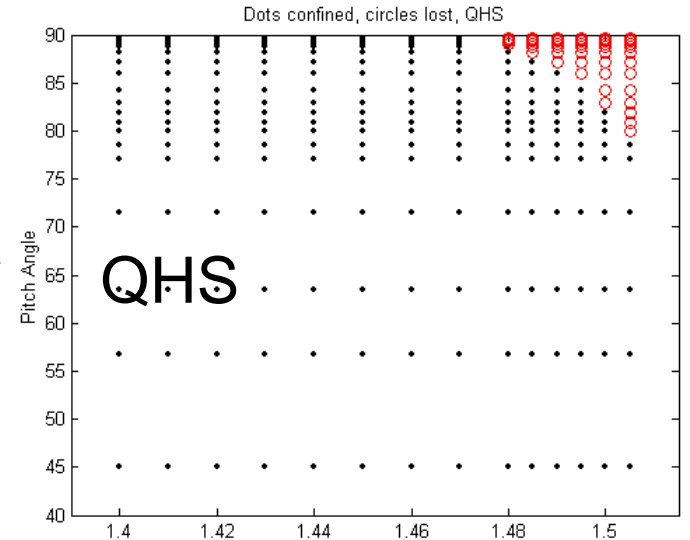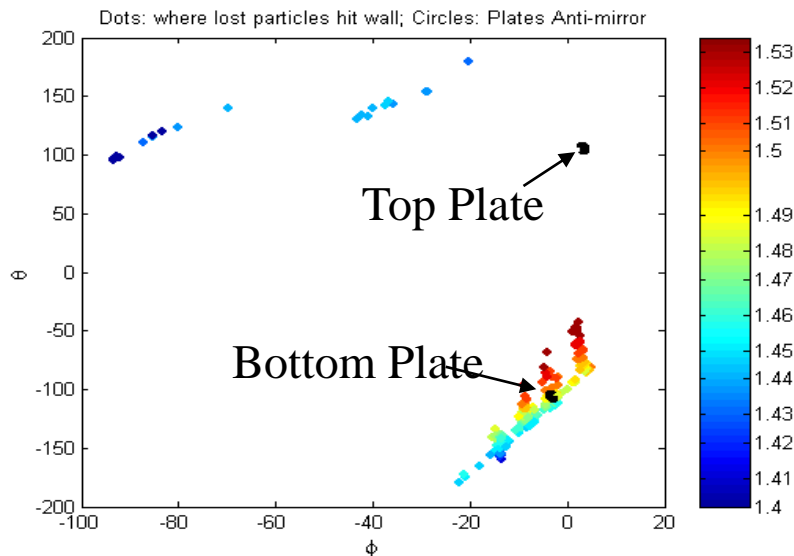
n_e (1×10^{13} cm^{-3})

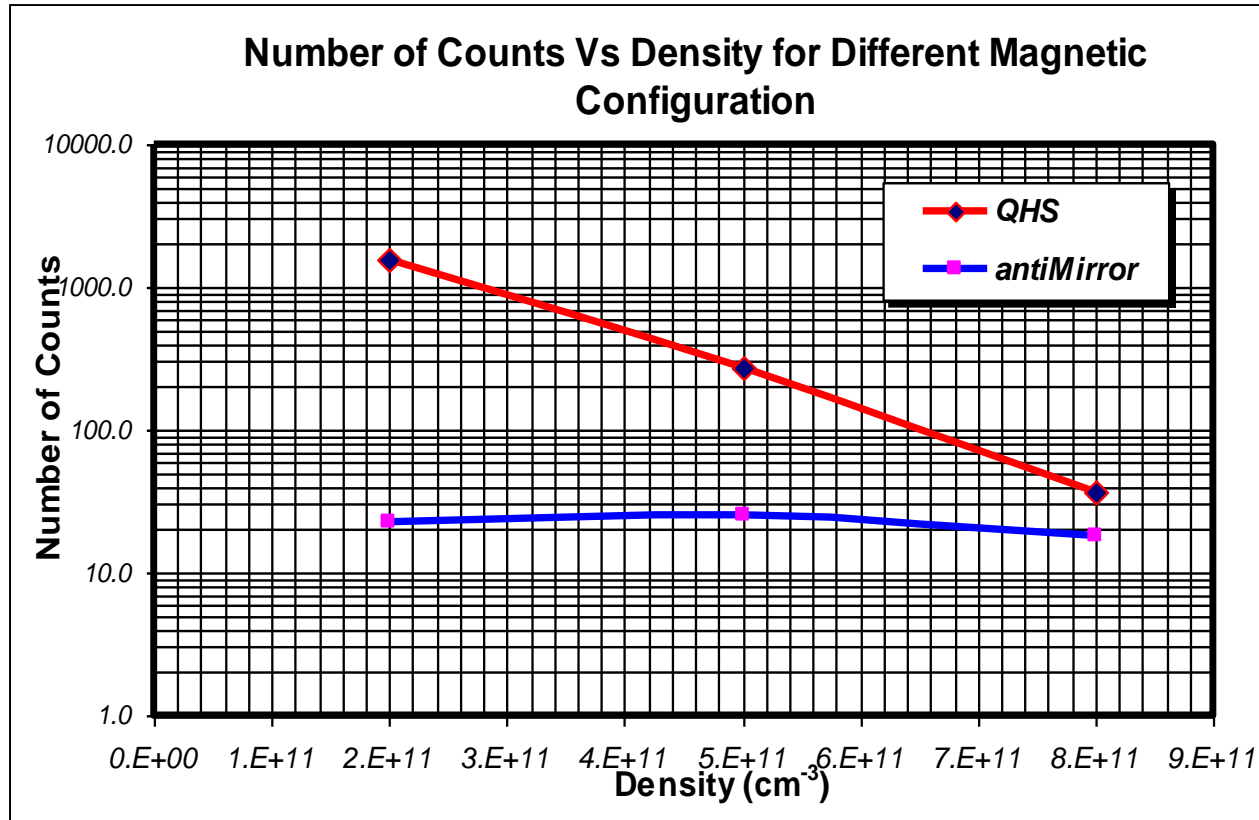The phenomenon appears to be due to direct loss orbits.

Modeling Confirms Direct Loss Explanation

- Confinement of single particle orbits vs. pitch angle and launch location.
- Black: Confined Orbit.
- Red: Lost Particle

Plates are at Location Where antiMirror Loss Orbits Hit the Wall

Dots: where lost particles hit wall; Circles: Plates Anti-mirror

Top Plate

Bottom Plate

Dots confined, circles lost, QHS

QHS

Dots confined, circles lost, Anti-mirror Anti-clockwise

antiMirror

Axis   LCFS

Hard X-ray Flux is Drastically Reduced in the antiMirror Configuration

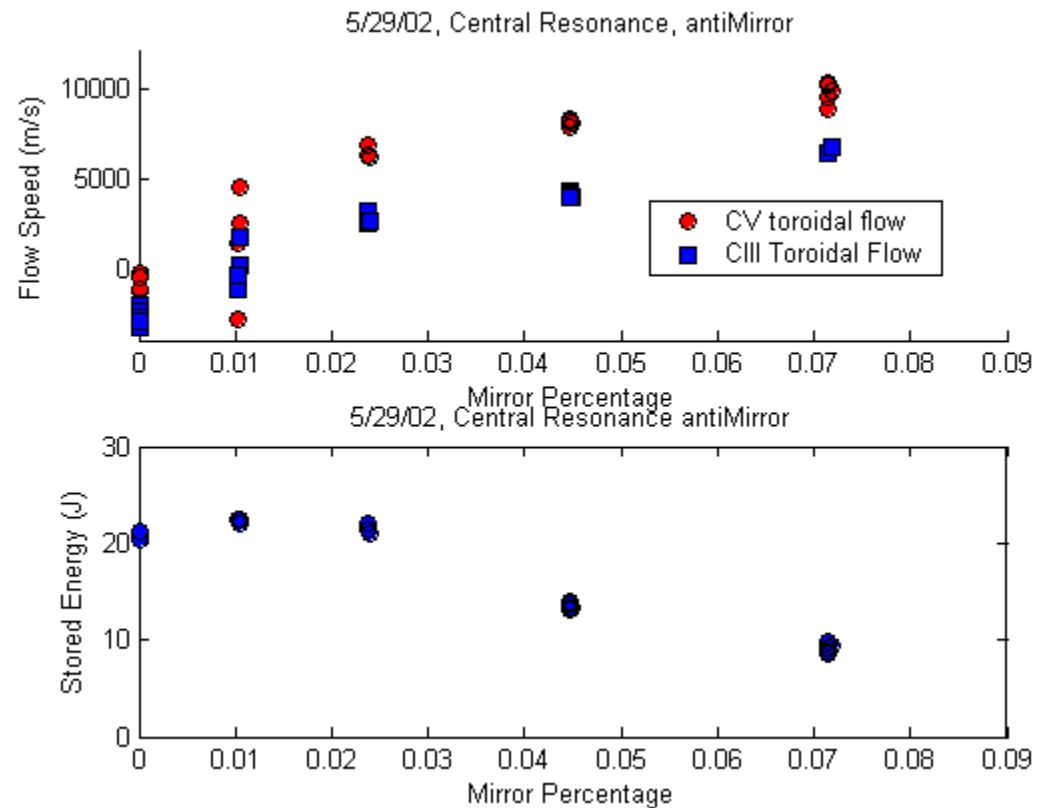**Number of Counts Vs Density for Different Magnetic Configuration**

- Pulses measured with a CdZnTe PHA system, with energy range from 50keV to 1MeV.
- Difference of 2 orders of magnitude in the hard X-ray flux at low density.

Impurity Toroidal Velocity Increases as the antiMirror Amplitude Increases.

- Increase in Toroidal C-V velocity and Decrease in Stored Energy Observed as the antiMirror amplitude is increased.

- Measurements made at a density of 1×10^{12} cm^{-3}, CH_4 doped plasma.

- Radial current of trapped electrons driving rotation?

5/29/02, Central Resonance, antiMirror

Legend: CV toroidal flow, CIII Toroidal Flow

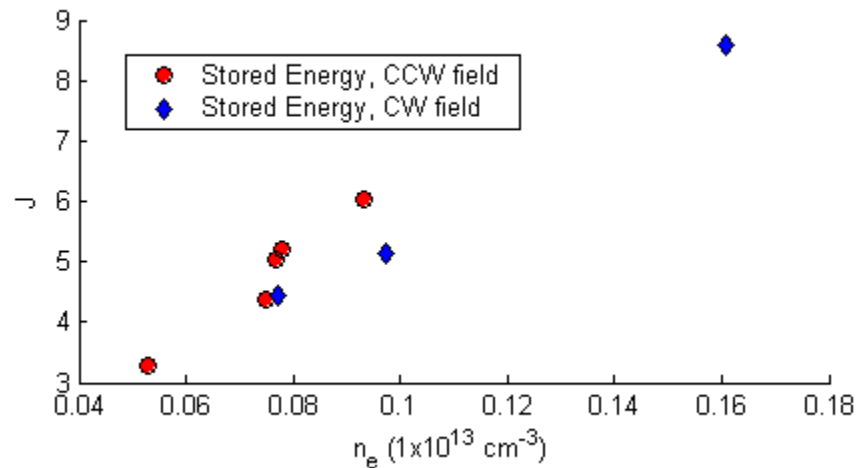5/29/02, Central Resonance antiMirror

Toroidal Flow Reverses Direction when the Magnetic Field is Reversed in antiMirror.

Rotation reverses when the field is flipped. Velocity is largely independent of the density. ⟶
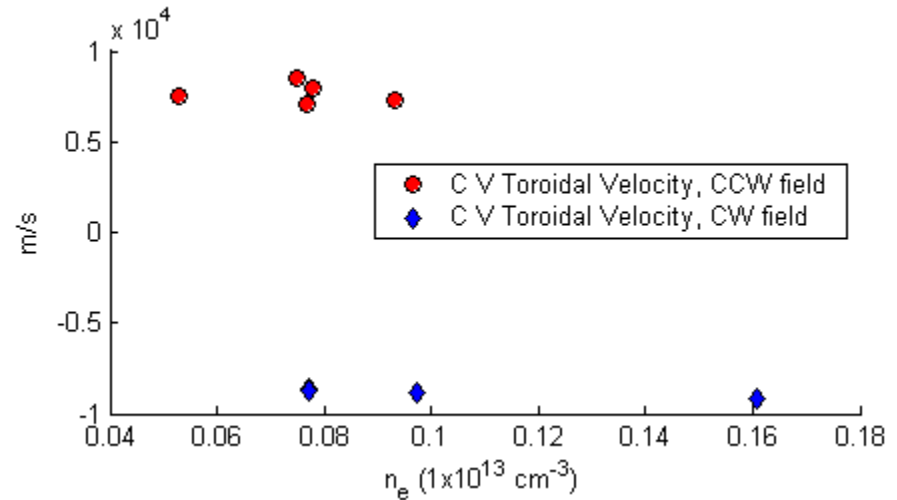
Stored energy increases with density for both field directions. ⟶

Conclusions

- Plasmas in HSX are heated with high ECH absorption efficiency to temperatures in excess of 600eV.

- The plasma is able to rotate more easily in the QHS configuration.

- Direct loss orbits are detected in configurations where symmetry is broken and deep minimum in |B| is at the ECH resonance location. This direct loss current may be driving rotation.

Presentation will be posted at hsxa.ece.wisc.edu.